Observations and Interpretations of Energetic Neutral Hydrogen Atoms from the December 5, 2006 Solar Event

R.A. Mewaldt*, R.A. Leske*, A.Y. Shih‡, E.C. Stone*, A.F. Barghouty¶, C.M.S. Cohen*, A.C. Cummings*, A.W. Labrador*, T.T. von Rosenvinge§ and M.E. Wiedenbeck†

*California Institute of Technology, Pasadena, CA 91125 USA
‡University of California, Berkeley, CA 94720 USA
¶NASA/Marshall Space Flight Center, Huntsville, AL 35812 USA
§NASA/Goddard Space Flight Center, Greenbelt, MD 20771 USA
†Jet Propulsion Laboratory, California Institute of Technology, Pasadena, CA 91109 USA

Abstract. We discuss recently reported observations of energetic neutral hydrogen atoms (ENAs) from an X9 solar flare/coronal mass ejection event on 5 December 2006, located at E79. The observations were made by the Low Energy Telescopes (LETs) on STEREO A and B. Prior to the arrival of the main solar energetic particle (SEP) event at Earth, both LETs observed a sudden burst of 1.6 to 15 MeV energetic neutral hydrogen atoms produced by either flare or shock-accelerated protons. RHESSI measurements of the 2.2-MeV γ-ray line provide an estimate of the number of interacting flare-accelerated protons in this event, which leads to an improved estimate of ENA production by flare-accelerated protons. Taking into account ENA losses, we find that the observed ENAs must have been produced in the high corona at heliocentric distances ≥2 solar radii. Although there are no CME images from this event, it is shown that CME-shock-accelerated protons can, in principle, produce a time-history consistent with the observations.

Keywords: energetic neutral atoms; solar energetic particles; flares, coronal mass ejections
PACS: 96.50.Vg; 96.50.Zc; 96.50.PW; 96.60.ph; 96.60.qe

INTRODUCTION

In early December of 2006, shortly after the launch of NASA's STEREO mission, and under near solar-minimum conditions, the Sun suddenly unleashed four X-class flares, each associated with a solar energetic particle (SEP) event. At this time the two STEREO spacecraft were still located close to Earth and many of the instruments were still being commissioned. Fortunately, the Low Energy Telescopes (LETs) and High Energy Telescopes (HETs) were already operational at the time of the first event, an X9 flare at 1019 UT on December 5. Since this event originated at E79 there was no direct connection to Earth along the interplanetary magnetic field and most of the energetic particles began arriving just after 1400 UT, ~4 hours after onset of the X-ray flare [1]. However, prior to the start of the main event both LETs observed a low-energy precursor, arriving between 1130 and 1300 UT.

Surprisingly, >70% of the particles during this precursor (identified by the LETs as protons with 1.6 to 15 MeV) were found to arrive from within ±10° longitude of the Sun, having apparently traveled directly across the interplanetary magnetic field (oriented 36° to 67° from the Earth-Sun line during this interval). After considering alternatives, Mewaldt et al. [1] concluded that the precursor was composed of energetic neutral hydrogen atoms (ENAs) created from protons accelerated by the December 5 flare and/or CME-driven shock. In LET the ENAs are stripped of their electron upon striking thin front Kapton windows. Solar ENAs therefore preserve their original direction until detection.

In this paper we review the December 5 observations, discuss ENA production and loss processes on the Sun, use RHESSI data to estimate ENA production by flare-accelerated protons, and compare estimated and measured yields of ENAs from both flare and shock-accelerated particles.

STEREO AND RHESSI OBSERVATIONS

Together, the STEREO LETs and HETs measure the nuclear charge (Z) and kinetic energy of H, He and heavier ions through Ni from ~2 to ~100 MeV/nuc. LET is composed of a double-ended array of 14 position-sensitive silicon solid-state detectors, including ten ~25-micron thick devices arranged in two fan-shaped arrays centered on a four-detector double-ended stack [2]. Particle directions are measured over 130° x 29° fans in the front and back directions with ~±6° maximum uncertainty in the ecliptic plane. The HET includes a stack of nine circular silicon solid-state detectors (1-mm thick) with a single-ended cone-shaped field of view with 55° full angle [3].

The ENAs in the precursor exhibited velocity-dispersion with higher-energy particles arriving first. Mewaldt et al. [1] used particles arriving from within ±10° of the solar longitude to derive the ENA emission profile using the measured kinetic energy (E) to derive particle velocity, $v = (2E/m)^{1/2}$, and the emission time, with m the proton mass. The emission profile is compared to the GOES X-ray profile in Figure 1. The similarity of the ENA and X-ray profiles confirms that the ENAs originated in this solar event. We consider here ENAs with 1.8 to 5 MeV, whose energy spectrum can be represented as a power-law with -2.5 slope (at higher energies, neutron-decay protons may contribute [1]). Assuming isotropic emission, an estimated 1.8 x 10^{28} ENAs with 1.8 – 5 MeV escaped the Sun [1].

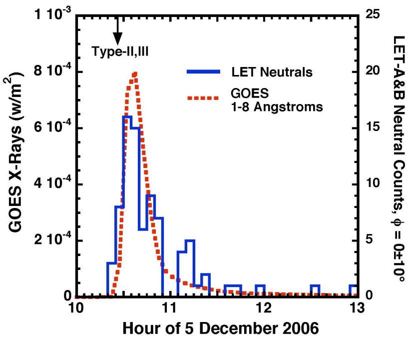

Figure 1: The derived emission profile of the ENA burst (in counts per 5 minutes) is compared with the 1-minute GOES X-ray profile and the onset of STEREO type-II and type-III radio bursts (adapted from [1]).

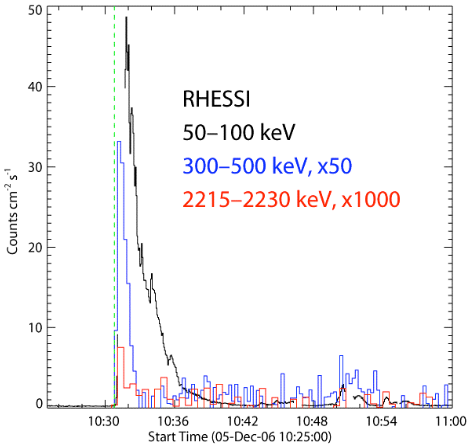

Figure 2: RHESSI light-curves for the December 5 flare in three energy bands, scaled for clarity. The 50–100 keV light-curve and 300–500 keV light-curve (background-subtracted) are primarily electron bremsstrahlung continuum emission, while the 2215–2230 keV light-curve (background-subtracted) is dominated by the 2.223 MeV neutron-capture line. The green dashed line shows when RHESSI came out of eclipse, indicating that it likely missed part of the emission. The 50–100 keV light-curve has data removed during high-deadtime periods.

RHESSI observed high-energy X-rays and γ-rays from this flare, although it missed the emission onset due to being in eclipse (soft X-ray emission in Figure 1 began at ~1019 UT and peaked at ~1035). The RHESSI observations start at ~1031 UT and the X and γ emission die out after a few minutes (Figure 2). This high-energy emission is mostly bremsstrahlung continuum produced by flare-accelerated electrons. A 2.223 MeV neutron-capture line was also produced by >~20 MeV/nuc flare-accelerated ions interacting with the lower chromosphere and producing neutrons that were captured at even greater depths (e.g., [4]).

RHESSI data can be used to estimate the number of flare-accelerated protons that underwent nuclear reactions in the solar atmosphere [5]. The neutron-capture line fluence at 1 AU determined from a spectral fit is $3.2\pm0.9 \times 10^{-2}$ photons/cm^2, which has been attenuated by Compton scattering in the solar atmosphere [6]. From *RHESSI* hard X-ray imaging, the 70-150 keV source was located 79.5° east of central meridian (S. Krucker, private communication). If the neutron-capture emission comes from the same location (this line cannot be imaged directly in this flare), the line flux is attenuated by 67%. Correcting for this loss and using neutron-capture line yields from simulations (R. Murphy, private communication), the observed fluence corresponds to 1.3×10^{31} interacting protons >30 MeV, for a proton spectral index of -3.5. If RHESSI missed some of the line emission, the number of interacting protons would be larger.

An independent limit of <3.1 x 10^{32} interacting protons was obtained [1] by assuming the 2-σ excess of 13-40 MeV protons observed by HET at this time was due to neutron-decay protons. The RHESSI limit is likely the better estimate as it is based on γ-ray data from the same event and uses up-to-date models.

ENA PRODUCTION AND LOSS

The timing of the ENA emission (Figure 1) suggests production by flare-accelerated protons. ENA H atoms are usually attributed to energetic protons that become neutral through charge-exchange with H or He. However, at coronal temperatures (1-2 MK) or in the flare site (3 – 30 MK [7]), there is not expected to be significant neutral H or He on which to charge exchange. ENAs are also produced by radiative recombination with free electrons ($H^+ + e \rightarrow H + \gamma$) with a cross section given by $\sigma_{rr} = 1.28 \times 10^{-25}\ E^{-2.0}\ cm^2$ (see [8]; with E in MeV). In addition, Mewaldt et al. [1] suggested that charge exchange with heavy coronal ions that retain some electrons is important (e.g., $H^+ + O^{6+} \rightarrow H + O^{+7}$). Lacking measurements of this or related cross sections they made theoretical estimates suggesting that heavy-ion charge-exchange processes (summed over coronal species) contributed ~150 times more than radiative recombination.

Following Mewaldt et al. [1] we assume all protons with <10 MeV slow and stop in the solar atmosphere. Using the RHESSI limit on 1.8-5 MeV protons and the production cross sections above we find that $>4 \times 10^{31}$ ENAs are produced with 1.8-5 MeV, >1000 times more than needed to explain the observations assuming isotropic emission and that all upward-moving ENAs escape the Sun. However, ENAs can be ionized by electron and proton impact ionization and by UV. At MeV energies the electron and proton ionization cross sections are equal and can be represented as $\sigma_i = 2.3 \times 10^{-17} \times E^{-0.895}\ cm^2$, with E the ENA energy in MeV [9]. Apart from $1/R^2$ attenuation, the attenuation factor $F(R) = \exp(-\sigma_i N_R)$ where N_R (in cm^{-2}) is the overlying column density of protons and electrons integrated from heliocentric distance R (at E79) to the STEREOs, using nominal coronal densities [10].

The production and loss of ENAs is illustrated in Figure 3. The solid curve plots the ENA production rate per accelerated 3-MeV proton (C_{ENA}) versus radius using $C_{ENA} = \sigma\ v\ N_T(R)$, where $N_T(R)$ is the number of targets per cm^3 at radius R, and σ is the species-weighted cross section for ENA production with coronal abundances [11]. The right hand scale plots the attenuation factor F(R) for 3-MeV ENAs that escape the Sun toward Earth from E79.

In the standard picture of a solar flare, magnetic reconnection suddenly releases a great deal of energy in the corona and energetic particles are quickly accelerated by one or more processes [12]. Aschwanden [12] estimated from X-ray studies that the height of the reconnection region varies from ~5,000 to ~50,000 km, with an extreme maximum of ~200,000 km (heliocentric radius ≈ 1.3 Rs). This process produces

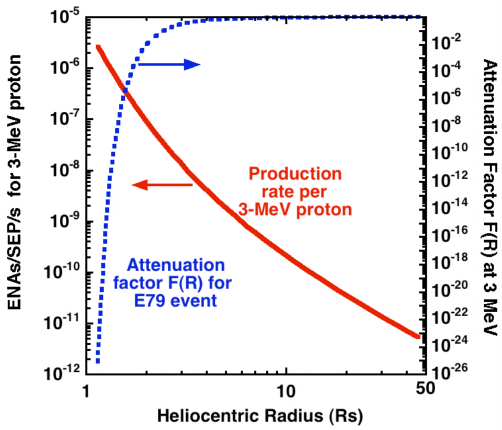

Figure 3: The solid curve (left axis) shows the ENA production rate per 3-MeV proton. The dotted curve (right axis) is the 3-MeV ENA attenuation factor, F(R).

upward and downward-moving proton and electron beams. Downward electrons produce bremsstrahlung in the chromospheric footpoints of the flare (Figure 2), while nuclear reactions of downward protons produce nuclear γ-rays, and also neutrons, which get captured to produce the 2.2 MeV n-capture line (Figure 2). The footpoints will be copious sites of ENA production because of neutral H and He in the chromosphere. However, only a very small fraction of ENAs from the chromosphere can escape the Sun (see Figure 3).

ENAs will also be produced in the acceleration region, but for a 3-MeV ENA from 1.15 – 1.3 Rs the attenuation factor ranges from 10^{-24} to 10^{-13}. Neither the acceleration site or flare footpoints should be observable in ENA emission at Earth for east-limb flares.

Flare-accelerated protons and electrons also move upward and a fraction escape into interplanetary space. To reconcile our ENA yield of 1.8×10^{28} with the RHESSI production estimate requires a mean ENA F(R) < 1000 (assuming half the energetic protons move upward) implying the observed ENAs are produced at >~2 Rs (see Figure 3). This could occur if some fraction of the upward-moving flare protons escape into the high corona and interplanetary space.

We now consider CME-shock accelerated particles. The type-II burst indicates formation of a coronal shock and the coincident type-III burst is due to electrons escaping the corona. There were no CME observations because SOHO/LASCO was undergoing routine maintenance and the STEREO coronagraphs were not yet commissioned. A summary of CME characteristics for 23 large SEP events had a median CME speed of 1800 km/s and median CME kinetic energy of 1.8×10^{32} ergs [13; see also 14]. Assuming these values and a CME launch at the 1019 UT X-ray onset, the CME would be at ~2.2 Rs when type-II emission started at ~1027, reaching 7 Rs ~30 min later.

For simplicity, we treat 1.8-5 MeV SEPs as three monoenergetic populations with 2.2, 3 and 4.2 MeV and relate the production rate of ENAs observed at Earth (S_{ENA}) to the number of accelerated particles, N_{SEP}, with $S_{ENA} = N_{SEP} C_{ENA} F(R)$. A strong, planar shock with a density jump of 4 will accelerate protons with $dJ/dE \propto E^{-1}$. If accelerated protons spend equal time on both sides of the shock, N_T is ~2.5 times nominal coronal densities. For simplicity, we assume accelerated protons are concentrated near the shock with an intensity independent of R from 2.2 to ~15 Rs. Figure 4 compares the normalized S_{ENA} rate with the observed ENA emission profile. The estimated profile is generally consistent with the LET observations.

As a cross check we estimate the energy content of the SEP spectrum producing the S_{ENA} curve in Figure 4. For $dJ/dE \sim E^{-1}$ the energy content of 0.04 - 30 MeV protons is ~6x that for 1.8 – 5 MeV (observed E^{-1} SEP spectra steepen before 30 MeV [15]). We find an SEP energy requirement of $E_{SEP} \approx 2 \times 10^{30}$ ergs neglecting SEPs that escape upstream. A study of 23 large SEP events [13] found the SEP energy content averaged ~10% of the CME kinetic energy. For our assumed $KE_{CME} = 1.8 \times 10^{32}$ ergs our estimated $E_{SEP} \approx 2 \times 10^{30}$ ergs is ~1% of the CME kinetic energy, not unreasonable for this prime acceleration region near the Sun, even allowing a factor of several for particles escaping upstream. A slower CME speed can be accommodated if CME launch was before 1019 UT.

SUMMARY AND CONCLUSIONS

RHESSI observations of the neutron-capture line give improved estimates of the flare-accelerated protons and ENA production in the 5 December 2006 flare. If flare-accelerated protons cause most of the ENA production they must be created at >2 Rs to escape the Sun in sufficient numbers, suggesting that escaping rather than trapped flare particles are more likely responsible. It is also shown that the observed ENA emission, if due to CME-shock accelerated particles, would only require a small fraction (few %) of the kinetic energy of the typical ~2×10^{32} erg CME associated with large SEP events. Furthermore, the profile and timing of the ENA emission is plausible for a 1500-2000 km/s CME. Detailed modeling of flare and shock-accelerated ENA production would be very helpful in interpreting these observations.

In the approaching solar maximum STEREO ENA and SEP observations from multiple points of view, aided by imaging from STEREO and RHESSI and by modeling, can provide a new window into solar particle acceleration and transport on the Sun by revealing in greater detail when, where, and how the relatively poorly known spectra of low-energy (<10 MeV) solar protons are accelerated, interact with solar matter, and escape from the Sun.

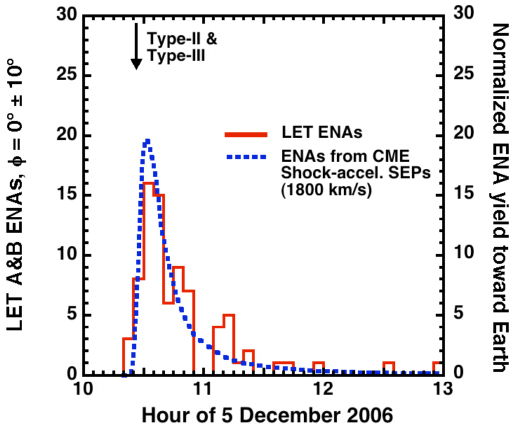

Figure 4: The estimated ENA emission profile for an 1800 km/s (constant) CME (dotted curve; see text) is compared with the profile observed by the STEREO LETs.

ACKNOWLEDGMENTS

This work was supported by NASA at Caltech and JPL under sub-contract SA2715-26309 from UC Berkeley under NASA contract NAS5-03131. The work at MSFC was supported by the TEI Program of NASA's Office of Chief Engineer. We thank NOAA for GOES X-ray data and appreciate discussions with Hugh Hudson, Sam Krucker, Gang Li, Bob Lin, Ron Murphy and Gerry Share.

REFERENCES

1. R. A. Mewaldt et al., *ApJ,* 693, L11, doi:10.1088/0004-637X (2009).
2. R. A. Mewaldt, et al., *Sp. Sci. Rev.,* 136, 285, doi:10.1007/s11214-0077-9288-x (2008).
3. T. T. von Rosenvinge, et al., *Sp. Sci. Rev.,* 136 (2008).
4. R. J. Murphy, et al.*, ApJS,* 168, 167 (2007).
5. A. Y. Shih, et al., *ApJ*, 698 L152 (2009).
6. X.-M. Hua, and R. E. Lingenfelter, *Solar Physics,* 107, 351 (1987).
7. U. Feldman, *Phys. Plasmas,* 3, (9), 3203 (1996).
8. L. H. Andersen, and J. Bolko, *Phys. Rev. A.*, 42, 1184 (1990).
9. A. F. Barghouty, *Phys. Rev. A*, 61, 052702 (2000).
10. E. C. Sittler, Jr., and M. Guhathakurta, *ApJ*, 523, 812 (1999).
11. U. Feldman, and K. G. Widing, *Sp. Sci. Rev.*, 107, 665 (2003).
12. M. A. Aschwanden, *Sp. Sci. Rev.* 101, 1 (2002)
13. R. A. Mewaldt et al., in *Particle Acceleration and Transport in the Heliosphere and Beyond*, G. Li, et al., eds, AIP Conf. Proc. 1039, 2008, p. 111.
14. N. Golpalswamy, *J. Astrophys. Astr*. 27, 243 (2006).
15. R. A. Mewaldt, et al. *JGR* 110, doi:10.1029/2005 (2005).